Published in final edited form as:
Dev Cell. 2009 January ; 16(1): 35–46. doi:10.1016/j.devcel.2008.12.002.

Scara5 is a Ferritin Receptor Mediating Non-Transferrin Iron Delivery

Jau Yi Li[1,*], **Neal Paragas**[1,*], **Renee M. Ned**[2], **Andong Qiu**[1], **Melanie Viltard**[1], **Thomas Leete**[1], **Ian R. Drexler**[1], **Xia Chen**[1], **Simone Sanna-Cherchi**[1], **Farah Mohammed**[1], **David Williams**[1], **Chyuan Sheng Lin**[1], **Kai M. Schmidt-Ott**[1,3], **Nancy C. Andrews**[4], and **Jonathan Barasch**[1,†]

1 *Renal Division, College of Physicans & Surgeons of Columbia University New York, New York, USA 10032*

2 *National Office of Public Health Genomics Center for Disease Control Atlanta, Georgia, USA 30329*

3 *Department of Nephrology and Hypertensiology, Charité Berlin, Campus Buch, Max-Delbrück Center for Molecular Medicine, 13125 Berlin, Germany*

4 *Pediatrics and Pharmacology, Duke University School of Medicine Durham, North Carolina, USA 27708*

Summary

Developing organs require iron for a myriad of functions, but embryos deleted of the major adult transport protein, transferrin or its receptor transferrin receptor1 (TfR1$^{-/-}$) initiate organogenesis, suggesting that non-transferrin pathways are important. To examine these pathways, we developed chimeras composed of fluorescence-tagged TfR1$^{-/-}$ cells and untagged wild type cells. In the kidney, TfR1$^{-/-}$ cells populated capsule and stroma, mesenchyme and nephron, but were underrepresented in ureteric bud tips. Consistently, TfR1 provided transferrin to the ureteric bud, but not to the capsule or the stroma. Instead of transferrin, we found that the capsule internalized ferritin. Since the capsule expressed a novel receptor called Scara5, we tested its role in ferritin uptake and found that Scara5 bound serum ferritin and stimulated its endocytosis from the cell surface with consequent iron delivery. These data implicate cell type-specific mechanisms of iron traffic in organogenesis, which alternatively utilize transferrin or non-transferrin iron delivery pathways.

Introduction

Iron travels from the placenta to embryonic organs bound to carrier proteins, such as transferrin, which is detectable in extracellular fluids by mid-gestation in rodents (Gustine and Zimmerman, 1973). Transferrin is then captured throughout the embryo by the transferrin receptor (TfR1). This pathway is essential for development, since deletion of *TfR1* resulted in embryonic death at E11-E12 (Levy et al., 1999). Indeed, during kidney development, transferrin was found to be both necessary and sufficient to stimulate tubulogenesis in vitro, suggesting a critical role for transferrin mediated iron transport in nephrogenesis (Ekblom et al., 1983) and by extension perhaps to the development of other organs. The widespread

†Corresponding Author Department of Medicine, 630 West 168th St, New York, NY 10032, T:212-305-1890, F:212-305-6874, E-mail: jmb4@columbia.edu.
*Equal contribution.

expression of TfR1 (Aisen, 2004) further reinforced the view that transferrin plays a critical role throughout the embryo.

A detailed analysis of specific embryonic lineages, however, suggests a more restricted view of the transferrin pathway. Transferrin is necessary for thymic maturation (Brekelmans et al., 1994; Ned et al., 2003; Macedo et al., 2004) but this requirement is stage specific, since TfR1 neutralizing antibodies block the progression of double negative thymocytes, but fail to inhibit earlier stages of the lymphoid lineage, despite the fact that TfR1 is expressed at all stages. Likewise, while $TfR1^{-/-}$ embryos (Levy et al., 1999) have specific defects in erythroid, lymphoid and spinal cord development, most other organs appear to initiate development. Chimeras composed of $TfR1^{-/-}$ and wild type ES cells can live into adulthood, and $TfR1^{-/-}$ cells can be detected by Southern blots in a variety of organs, confirming the notion that different cells can arise from $TfR1^{-/-}$ ES cells in vivo (Ned et al., 2003). Similarly, apparently normal organogenesis occurs in hypotransferrinemic mice$^{hpx/hpx}$ (Huggenvik et al., 1989; Trenor et al., 2000) and humans (Hayashi et al., 1993; Hamill et al., 1991), despite severe anemia. Hence, while specific stages of the hematopoeitic lineage (Kanayasu-Toyoda et al., 1999; Sposi et al., 2000; Wingert et al., 2004), bone (Gentili et al., 1994) and nervous system (Siddappa et al., 2002; Levy et al., 1999) depend on TfR1, other cells in the embryo may capture iron by a non-transferrin mechanism. However, few non-transferrin iron trafficking molecules are known, and knockouts of non-transferrin carriers including *Lcn2* (Flo et al., 2005) and iron uptake proteins such as *DMT1* (Gunshin et al., 2005) and *Steap3* (Ohgami et al., 2005) do not grossly disrupt organogenesis. These data leave many fundamental questions unresolved, such as the identity of other iron carriers, their receptors that deliver iron into an appropriate intracellular compartment, and whether different pathways of iron delivery are cell specific.

Ferritin is a major iron storage protein. Intracellular ferritin is composed of 24 subunits of L- and H-chains in varied proportion (Arosio et al., 2002). On the other hand, extracellular (serum) ferritin is composed mostly, but not exclusively of L-ferritin (Linder et al., 1996; Ghosh et al., 2004). Secretion of L-ferritin has been carefully documented in cell cultures (Tran et al., 1997; Ghosh et al., 2004) and in syndromes which over-express L-chain, such as heterozygous H chain-deficient mice (Ferreira et al., 2001), *hpx/hpx* mice (Simpson et al., 1991; Dickinson et al., 1995), and humans with hyperferritinemia and cataracts (Beaumont et al., 1995). Cytokine stimulation of some cell types also induces H-ferritin secretion (Tran et al., 1997), particularly from macrophages (Chen et al., 2005; Recalcati et al., 2008). While the two chains of ferritin have complementary functions [H-ferritin is a ferroxidase (Levi et al., 1988) and L-ferritin induces polynucleation of iron (Levi et al., 1994)], both ferritins can independently incorporate iron into a core. For example, while serum-ferritin is iron poor compared to intracellular ferritin it contains 7 iron atoms/molecule (Wantanabe et al., 2001), similar to bacterially expressed L-ferritin, which contains 5–15 iron atoms/molecule (Levi et al., 1989, 1992). In the presence of even a single H chain, up to 4500 iron atoms can be incorporated into L-ferritin cages.

Extracellular ferritin can deliver iron to a variety of cells. Ferritin can bind cell surface receptors, undergo endocytosis and transfer of iron in sufficient quantities to alter iron dependent gene expression (Ponka et al, 1998). A receptor for H-ferritin has been identified, Tim2 (or Timd2; Chen et al., 2005), but its expression is highly restricted in the embryo. In contrast, receptors for L-ferritin have not been documented, but may in fact be particularly relevant in the embryo, whose serum ferritin concentration is 3–8 fold greater than that of maternal blood (Bratlid et al., 1980; Hussain et al., 1977; MacPhail et al., 1980; Puolakka et al., 1980).

To clarify the mechanisms of iron delivery in embryogenesis, we developed an in vivo assay to evaluate the requirement for TfR1. We focused on the embryonic kidney where cell type

progression is dependent on iron delivery (Ekblom et al., 1983). Using chimeric embryos composed of Green-Fluorescent Protein-labeled TfR1$^{-/-}$ cells (GFP-TfR1$^{-/-}$ cells) und unlabeled wildtype cells, we found that mesenchymal, stromal, and capsule compartments were robustly populated by GFP-TfR1$^{-/-}$ cells and accumulated iron independently of TfR1. Capsular cells expressed Scara5 (Jiang et al., 2006) which we found bound extracellular ferritin, mediated its endocytosis, and captured its iron. Tips of the branching ureteric bud on the other hand were poorly populated by GFP-TfR1$^{-/-}$ cells, confirming a cell type-specific, rather than a global requirement for transferrin-TfR1. These data imply that different mechanisms deliver iron to different cell types in the developing kidney.

Results

Evidence for Transferrin and Non-transferrin Iron Delivery in Kidney Development

The developing kidney is generated from three cellular lineages, epithelial (including the nephric duct, ureteric bud (UB), and collecting ducts), metanephric mesenchyme (composed of cap mesenchyme, pretubular aggregate, renal vesicle, C-and S-shaped bodies and nascent nephron) and a stromal compartment (composed of the capsule, cortical and medullary stroma). The ureteric bud generates a branched collecting duct system. The mesenchymal lineage converts to epithelia and gives rise to both mesonephric and metanephric nephrons, containing glomeruli and epithelial tubules. Capsular and stromal cells form the outermost rings of cells in the kidney cortex, and are composed of a variety of cells that have yet to be fully defined (Dressler et al., 2006; Hatini et al., 1996; Levinson and Mendelsohn, 2003; Schmidt-Ott et al., 2006).

To investigate pathways of iron delivery in the developing kidney, we first inspected TfR1$^{+/-}$ × TfR1$^{+/-}$ crosses (Levy et al., 1999; Ned et al., 2003). We examined 210 E11 embryos recovering TfR1$^{+/+}$ (28%), TfR1$^{+/-}$ (52%), and TfR1$^{-/-}$ (20%) in approximate Mendelian ratios. TfR1$^{-/-}$ embryos contained the Wolffian duct and associated mesonephric tubules (Figure 1A). The embryos also developed ureteric buds from the Wolffian duct (marked by creating Tfr1$^{-/-}$; Hoxb7-GFP^{+} lines; Srinivas et al., 1999) as well as cap mesenchyme (Figure 1B). In rare, surviving embryos at E11.5, elongated T-shaped UBs and renal vesicles were found (Supplemental Figure 1), but more advanced ureteric branching and mesenchymal-epithelial development could not be assayed due to the lethality of TfR1 knockout.

To determine whether TfR1$^{-/-}$ renal progenitors were competent to form organotypic structures, we used an in vitro culture system. As shown in Supplemental Figure 2, when TfR1$^{-/-}$ urogenital sheets (E11) were explanted and the media were supplemented with ferric ammonium citrate (20 μg/ml), a TfR1 independent iron donor, the sheet consistently generated highly branched ureteric buds surmounted by cap mesenchyme (n=21 urogenital sheets), whereas culture with transferrin resulted in regression of the tissue. This implied that urogenital progenitors, present in vivo when the sheet was explanted (E11) remained competent to form kidney specific structures despite the deletion of TfR1.

To test the functional requirement for transferrin in vivo beyond the E11 stage, we created chimeric embryos by injecting TfR1$^{-/-}$ ES cells into wild type blastocysts. TfR1$^{-/-}$ ES cells (Ned et al., 2003) were labeled by targeting the Rosa26 locus with GFP (Srinivas et al., 2001) and two different clones were utilized in subsequent experiments. The knock-in of GFP was confirmed by Southern blotting, and the deletion of TfR1 was confirmed by a series of assays that included genotyping, measuring cell surface TfR1 protein with CD71 antibodies, and incubation with Alexa568-transferrin, which showed that GFP targeted TfR1$^{-/-}$ ES cells neither expressed TfR1 nor captured transferrin (Supplemental Figure 3).

The GFP-TfR1$^{-/-}$ cells populated many embryonic organs including lung, liver, mid-gut, kidney, bladder and gonad, and within these tissues, GFP-TfR1$^{-/-}$ produced both epithelia (including branching and sheet structures) and mesenchymal precursors (Supplemental Figure 4), demonstrating the multipotency of the GFP-TfR1$^{-/-}$ cells.

In the kidney, we found extensive chimerism in the Wolffian ducts and the metanephric mesenchyme, as expected from our observation of early kidney structures in TfR1$^{-/-}$ embryos at E11.5 (Supplemental Figure 5). At the E15 stage, GFP-TfR1$^{-/-}$ cells were also present throughout the kidney (Figure 2, Supplemental Figure 5; n=14 total foster mothers, using two clones of GFP-TfR1$^{-/-}$ ES cells). To examine the contribution of the GFP-TfR1$^{-/-}$ cells to individual compartments, we compared the percentage of GFP^{+} cells found in each compartment, to the relative size of the compartment, measured by planimetry. The GFP-TfR1$^{-/-}$ cells populated distal tubules (identified by staining for E-cadherin; median ratio= 1.7; p=0.0001), proximal tubules (which stained with lotus lectin; median ratio=1.930; p=0.0425) and the stroma and capsule contained as much as 42%±17% of the GFP-TfR1$^{-/-}$ cells (median ratio=4.1; p<0.001), even though these compartments account for only 6–9% of the cells in the E15 kidney (as estimated by FACS analysis of kidneys expressing Foxd1-GFP). In contrast to these findings, cortical tips of the ureteric bud (highlighted by the expression of both E-cadherin and Troma1) contained the fewest GFP-TfR1$^{-/-}$ cells (median ratio=0.43; p=0.003), even in kidneys with high overall degrees of chimerism (Figure 2, Supplemental Figures 5 and 6). The exclusion of GFP-TfR1$^{-/-}$ cells from the UB tip contrasted with chimeras generated with GFP-TfR1$^{+/+}$ ES cells, which populated all compartments including UB tips (TfR1$^{-/-}$ vs TfR1$^{+/+}$ p=0.78; Supplemental Figure 7).

To confirm the anatomical distribution of GFP-TfR1$^{-/-}$ cells, we used FACS to separate GFP-TfR1$^{-/-}$ from wild type cells using two different sets of kidneys (E15) with high degrees of chimerism (~60%) and measured gene expression using Affymetrix arrays (Mouse Genome 430 2.0). In agreement with prior studies (Levy et al., 1999; Ned et al., 2003), GFP-TfR1$^{-/-}$ cells were incompetent to participate in erythroid and granulocytic lineages: erythroid (*hemoglobin, aminolevulinic acid synthase 2*) and granulocytic (*lactoferrin, neutrophil granule protein*) genes were reduced on average 14-fold in GFP-TfR1$^{-/-}$ compared to TfR1$^{+/+}$ cells. Similarly, genes preferentially expressed by ureteric bud tips (*Wnt11, Wnt9B, Cytokine Receptor Like Factor1, Ros1*; Kanwar et al., 1995; Kispert et al., 1996; Marose et al., 2008; Schmidt-Ott et al., 2005) were decreased to 0.35±0.27 fold (TfR1$^{-/-}$ vs TfR1$^{+/+}$). On the contrary, genes expressed in renal stroma (*FGF-7, SFRP1, Semaphorin3A, Glypican3, FoxD1, Angiotensin II receptor, type 2*) and capsule (*Col6a1, Col5A2, Nfix*) were increased 2.9±0.8 and 2.7± 0.26 fold, in GFP-TfR1$^{-/-}$ vs TfR1$^{+/+}$ cells, respectively. These data were extended by analyzing a series of genes restricted to UB tip, stalk or the mesenchyme-stroma compartment, that we identified by expression profiling (Schmidt-Ott et al., 2005). This comparison showed markedly reduced expression of the top 200 ureteric tip-specific genes in GFP-TfR1$^{-/-}$ cells isolated from E15 chimeric kidneys, when compared with the TfR1$^{+/+}$ population (0.42 fold; p=0.0000921; Fig. 2E). In contrast, the expression of the top 200 UB stalk-specific genes was only slightly reduced (0.71-fold; p=0.00265), while the expression of the top 200 mesenchymal-stromal specific genes was unchanged (1.2 fold; p=0.253; Figure 2F). These data confirmed the preferential location of GFP-TfR1$^{-/-}$ cells in mesenchyme and stroma, particularly compared to ureteric tip.

While it may be the case that the surviving GFP-TfR1$^{-/-}$ cells were severely iron deficient, this was unlikely because, as shown in Figures 2G, they displayed cytoplasmic iron stores (intracellular ferritin). In addition, GFP-TfR1$^{-/-}$ cells demonstrated only slightly reduced proliferation (as detected by phospho-histone H3 staining median ratio=0.69, p=0.0051) compared to neighboring wild type cells, and the same frequency of apoptosis (as detected by activated caspase-3 staining; p=0.26). These findings imply that GFP-TfR1$^{-/-}$ cells were not

severely iron starved. Yet, in situ, these cells failed to capture Alexa568-transferrin (Figure 2H), implying that they did not express an alternative transferrin receptor. These data suggested that transferrin-independent mechanisms of iron capture were active in GFP-TfR1$^{-/-}$ cells.

Endocytosis of Transferrin and Ferritin by Different Cellular Compartments in Developing Kidney

Extracellular ferritin is a non-transferrin iron carrier that is endocytosed by a variety of cells, including squamous-like cells of the adult kidney capsule (Kobayashi, 1978). To investigate ferritin capture by embryonic kidney, we incubated E15 kidneys with Alexa568–apo-ferritin, and found prominent endocytosis of ferritin by capsular cells. The capture of ferritin was independent of TfR1 because both wild type and GFP-TfR1$^{-/-}$ cells captured ferritin (Figure 3A and B). Ferritin L-chain was recognized by the cells, because the pattern of uptake was reproduced by L-, but not by H-ferritin. To determine whether ferritin transferred its iron to the cell cytoplasm we incubated explanted kidneys in the presence of either iron-loaded ferritin (holo-ferritin) or iron-deprived ferritin (apo-ferritin) and assayed proliferation in the capsular region. When holo-ferritin was administered to explanted kidneys, 49% of capsular nuclei expressed the proliferation marker phospho-histone H3, whereas apo-ferritin induced labeling in only 12% of nuclei ($p=0.04$; Figure 3C, D), implying that ferritin-mediated iron delivery determined the cellularity of the renal capsule. Consistently, prominent staining for endogenous ferritin (Figure 3E) implied ongoing iron accumulation in the capsule in vivo.

Ferritin uptake was quite different from that of transferrin. TfR1 was largely restricted to the ureteric bud, cap mesenchyme, and primitive nephron (Fig 4 A-C), identical to sites where transferrin was captured (Figure 4D). In contrast, capsule and stroma demonstrated limited endocytosis of transferrin, even though they were capable of endocytosis of fluid phase fluorescent dextran (Figure 4E). These results demonstrate that ferritin and transferrin receptors are both present in developing kidney, but that they mediate iron transport to different cell types.

Identification of a Novel Ferritin Receptor

The robust chimerism of GFP-TfR1$^{-/-}$ in the stroma and capsule suggested that they must capture non-transferrin iron, perhaps including ferritin. To examine this possibility, we isolated GFP-TfR1$^{-/-}$ cells by FACS and profiled their gene expression. We found that 156 genes were consistently upregulated $\geq$2 fold in the GFP-TfR1$^{-/-}$ population compared with TfR1^{+} cells (Geo Accession Number, GSE739), but only one of these, *scavenger receptor, member 5* (Scara5) was markedly upregulated (7.1 fold in GFP-TfR1$^{-/-}$ vs TfR1$^{+/+}$; $p=0.0011$) and shown by in situ hybridization to be specifically located in a rim of cells where ferritin was captured in both embryonic (Figure 3F) and adult kidney (not shown). Scara5 was also present in the airway, the developing aorta and muscle bundles, and it was heavily expressed by gonadal epithelia (Supplemental Figure 8; Jiang et al., 2006).

To directly test whether ferritin might be a ligand for Scara5, we expressed V5-tagged Scara5 in Trvb cells, a cell line that lacks endogenous expression Scara5 and Tfr1 (McGraw et al., 1987). Transiently transfected cells internalized apo-ferritin (Figure 5A), while Trvb cells transfected with a control vector did not (data not shown). Trvb clones (D2 and H2) that stably over-expressed Scara5 also demonstrated enhanced ferritin uptake compared to parental cells (Figure 5B) or clones (B2) that failed to express the protein. Western blots of these clones showed that Scara5 was present as 59KDa and 70KDa proteins (Figure 5C), suggesting post-translational processing.

To demonstrate that Scara5 binds ferritin at the cell surface, we added native ferritin at 4°C to MSC-1 cells overexpressing V5-tagged Scara5. Using two-color immunofluorescence, we

found immunodetectable patches of V5 and ferritin on the surface of non-permeabilized cells (Figure 6A). Raising the temperature to 37°C resulted in endocytosis of the ferritin, while inclusion of 100 fold excess unlabelled ferritin blocked both binding and endocytosis (Figure 6B). Scara5 co-immunoprecipitated from clones D2 and H2 together with ferritin-avidin, but not with avidin itself (Figure 6C). Immunoprecipitation with ferritin-avidin coated biotin beads pulled down immunodetectable Scara5, but avidin-coated biotin beads did not (Figure 6D). These data indicate that Scara5 and ferritin interact at the cell surface.

It is well-known that scavenger receptors bind more than one ligand, however to our knowledge iron-transporting proteins had not been shown to bind to this class of receptors. Using our stable Scara5-Trvb clones, we studied whether Scara5 recognized a variety of iron carriers. L-ferritin was the preferred ligand; addition of as little as 250pmole of L-chain (equivalent to 10 pmoles of an L-chain complex) in the media led to detection of ferritin in cellular vesicles of H2 and D2 clones but not in parental Trvb cells nor in non-expressing clone B2 (Figure 5D). Scavenger receptors bind to their ligands using electrostatic interaction. Because attachment of fluorescent probes to ferritin might have altered its net charge, we tested ferritin attached to two fluorophores, Alexa-568 which adds a negative charge and Alexa488 and Rhodamine which adds a positive charge. The uptake of these two types of ferritins resulted in similar levels of Scara5 dependent endocytosis. Haptoglobin-hemoglobin was also internalized by H2 and D2 clones, but the signal was less distinct than that of L-ferritin (Supplemental Figure 9). H-ferritin, in contrast, was not captured, nor were transferrin, albumin, hemopexin-heme or lipocalin2:catecholate siderophore. Further, Scara5 differed from other scavenger receptors since it did not capture fluorescent acetylated LDL (Jiang et al., 2006). These data suggest that among other potential ligands, Scara5 is a receptor or a component of a receptor for L-ferritin.

Scara5 Expressing Cells can Obtain Iron from Ferritin

To examine whether Scara5 can deliver iron to the cell, we incubated Scara5 expressing D2 and H2 clones with ferritin loaded with radioactive iron and found that there was a time dependent incorporation into the Scara5-expressing cells, but not into the parental Trvb cell (Figure 7A). Iron was likely obtained after endocytosis into an acidic compartment, because 4°C or inhibition of vacuolar H^+ATPase with bafilomycin blocked iron capture and ferritin traffic to lysosomes (Figure 7A, B). Consistent data came from a MSC-1 reporter cell line which expressed endogenous Scara5 as well as fluorescent proteins driven by iron responsive elements (IRE, Li et al., 2004). Holoferritin upregulated CFP encoded by a 5′ IRE reporter gene, and down regulated YFP encoded by a 3′ IRE reporter gene, consistent with the transfer of iron to the cytoplasm (Figure 7C). In the presence of holoferritin (2 μg/ml), the 5′ IRE/3′ IRE fluorescence ratio (1.58±0.31) was not significantly different (ratio=3.8±1.5; p=0.19) from that of cells incubated in media containing ferric ammonium citrate (50 μM) and holotransferrin (20 μg/ml). Cells incubated in media containing the iron chelator, desferroxamine (20 μM) had a significantly lower ratio (0.53±0.09; p=0.044) than cells incubated with holoferritin. To test whether ferritin iron can enhance cell survival under iron-limiting conditions in a Scara5-dependent manner, we incubated clones (D2 or H2) in minimal iron-deficient media supplemented with either holo- or apo-ferritin. Whereas Trvb cells were unresponsive to either protein (n=8), holo-ferritin, but not apo-ferritin, dose-dependently supported the survival of Scara5 expressing cells as measured by GAPDH blots (Figure 7D). Together, these data show that ferritin can deliver iron and regulate iron-dependent intracellular events in a Scara5-dependent manner.

Scara5 is an Endogenous Ferritin Uptake Pathway

To determine whether native Scara5 acts as a ferritin receptor, we suppressed its message in MSC-1 cells by RNA interference. We derived stable clones expressing short hairpin RNA (shRNA) targeting Scara5 and then transfected these clones with Scara5 siRNA (Qiu et al.,

2006). This protocol reduced Scara5 message to 29± 3.0%. Control studies showed that LacZ shRNA plus LacZ siRNA did not restrict the expression of Scara5 (110.5± 0.26% compared to non-transfected MSC-1 cells). The interference with Scara5 expression inhibited fluorescein-ferritin endocytosis, measured by FACS (61±0.1% compared to LacZ targeted cells; n=5; p=0.00093).

Chemical blockade of Scara5 with polyanions further confirmed the interaction with ferritin. Polyinosinic acid (PI; 50 μg/ml) nearly abolished the capture of Alexa488-ferritin by MSC-1 cells, whereas polyguanylic acid (PG) and polycytidylic acid (PC) were less effective (Figure 7E) as previously demonstrated for other ligands by Jiang et al., 2006. Consistently, the transfer of iron from holo-ferritin to MSC-1 cells was inhibited by PI, suppressing the ratio of iron reporters 5′ IRE-CFP/3′ IRE-YFP (0.7±0.06; holoferritin vs holoferritin+PI p=0.05) whereas PC was ineffective (1.2±0.2; holoferritin vs holoferritin+PC p=0.4). In contrast, PI did not block the response of the iron reporters to ferric ammonium citrate (data not shown). To demonstrate that this behavior was not unique to the MSC-1 cells, we repeated the inhibition studies in clones D2 and H2 and in explanted kidneys and found similar results. In aggregate, our data demonstrate that Scara5 can act as a ferritin receptor delivering iron to the cytoplasm where it activates iron responsive elements.

Discussion

While iron transport to developing organs is critical, the molecules that mediate this process remain poorly understood. Genes that deliver iron to some lineages do not seem to be needed throughout the embryo. For example, $TfR1^{-/-}$ cells can populate developing organs (Ned et al., 2003), $DMT1^{-/-}$ mice still undergo hepatic organogenesis (Gunshin et al., 2005), and mutations in Steap3 (Ohgami et al., 2005) are compatible with development. The candidate iron carrier Lcn2 is not essential in development and was even downregulated in the GFP-$TfR1^{-/-}$ cell population, suggesting that it can not compensate for $TfR1^{-/-}$.

To determine the mechanism of iron delivery in the embryonic kidney, we first examined the transferrin pathway. The most striking finding was a restricted requirement for TfR1. For example, thousands of differentiated kidney, gonad, bladder, mid-gut, liver and lung cells were generated from only 3–5 GFP-$TfR1^{-/-}$ ES cells, implying that expression of TfR1 was not required at any step of their lineage. In fact, we failed to visualize an interaction of transferrin with GFP-$TfR1^{-/-}$ cells (Thorstensen et al., 1995), suggesting that they did not express an uncharacterized transferrin receptor, although chimeric embryos in the *hpx* background must be generated to formally test this idea. It also remained possible that iron was supplied from immediately adjacent $TfR1^{+/+}$ mesenchyme or epithelia, but this idea was effectively ruled out by the large clusters of differentiated GFP-$TfR1^{-/-}$ cells encompassing entire kidney compartments (Figure 2A, D, H; Supplemental Figure 5D, R, BB, 5F). In sum, we found that TfR1 did not limit the development of mesenchyme, nephron, stroma or capsule cells, most likely because of transferrin independent pathways. In fact, when we introduced ^{55}Fe during pregnancy (E11.5 or E12), ^{55}Fe was uniformly distributed at E12.5 (Supplemental Figure 10) despite variations in the expression of TfR1, again implicating one or more non-transferrin mechanisms of iron delivery in the kidney.

Extracellular ferritin may be a non-transferrin source of iron. First, while serum ferritin is not thought to be a major iron carrier in the adult, its concentration is nearly 3–8 fold higher in fetal blood than that of the mother (approximately 0.3 μg/ml; Puolakka et al., 1980; Siddappa et al., 2007) and it has the potential to carry a larger number of iron atoms/molecule than transferrin (Wantanabe et al., 2001; Levi et al., 1989, 1992). Second, extracellular ferritin may be synthesized locally by macrophages (Leimberg et al., 2008; Yaun et al., 2004) which are abundant in metanephric mesenchyme (Rae et al., 2007). During kidney development, 25% of

mesenchymal cells undergo apoptosis, and 3% of kidney cells are apoptotic at steady state (Koseki et al., 1992). While apoptotic cells can be cleared by a number of cell types, there is evidence for macrophage involvement in the kidney (Camp et al., 1996). Hence, ferritin may derive from serum, but may also be obtained locally from macrophages, recycling iron from apoptotic cells.

The capture of ferritin was originally demonstrated in hepatocytes (Mack et al., 1983; Sibille et al., 1989), intestine (San Martin et al., 2008), white matter (Hulet et al., 1999), lymphoid cells (Moss et al., 1992), erythroid precursors (Meyron-Holtz et al., 1999) and in the capsule of the adult kidney (Kobayashi, 1978). In all of these cell types, ferritin used an endocytic pathway (Hulet et al., 2000; Gelvan et al., 1996; Bretscher and Thomson, 1989) and delivered iron to the cytoplasm (Radisky and Kaplan, 1998; San Martin et al., 2008). Our studies have added stroma of embryonic capsule to this long list of cells.

Scavenger receptors bind their ligands using a series of positively charged residues in the collagenous (Doi et al., 1993) or cysteine-rich domains (Ojala et al., 2007). Using these residues they bind lipopolysaccharides, bacteria, and polynucleotides all of which share repetitive polyanionic motifs (Jiang et al., 2006). While iron carriers have not been studied as ligands for scavenger receptors, ferritin contains repeating chains of polyanionic monomers, and like classical polyanionic ligands, its binding was sensitive to polynucleotides. In this light, it is important to determine whether ferritin binds to more than one scavenger receptor, or is uniquely bound by Scara5, particularly given that Scara5 appears not to bind the typical ligands, such as acetylated or oxidized LDL. Moreover, Scara3 (Han et al., 1998) which was also expressed in renal stroma and capsule, did not capture ferritin (data not shown). Hence, while we present data demonstrating a Scara5-ferritin interaction, it is unresolved whether Scara5 is a unique ferritin receptor component, or rather simply an example of a common scavenger-ferritin interaction.

A number of functions may be served by a Scara5-ferritin interaction, in addition to supplying iron to the cell hosting the receptor. These include transporting iron across a cellular layer. The best studied models of iron transcytosis is the duodenal cell, which provides ferroportin-dependent iron export. In an analogous fashion, brain capillary cells (Fisher et al., 2007; Xu and Ling, 1994) and placenta can also transfer iron, in fact from ferritin, through ferroportin (Lamparelli, 1989; Bastin et al., 2006). The renal capsule includes c-kit^{+}flk^{+}podocalyxin^{+} nascent capillaries (Schmidt-Ott et al., 2006) which may enhance delivery of serum ferritin, while their expression of ferroportin may export iron to adjacent stromal and mesenchymal cells. Perhaps transcellular transport provides iron to developing organs at critical stages prior to the completion of the vascular tree. While such a mechanism remains speculative, it is supported by the co-expression of Scara5 and ferroportin in mesenchyme that surrounds proximal lung buds and by the expression of Scara5 and ferroportin in thin layers of cells that surround other developing organs.

In contrast to the widespread development of GFP-TfR1$^{-/-}$ stroma, mesenchyme, and epithelia, we found limited development of GFP-TfR1$^{-/-}$ in ureteric tips, suggesting their dependence on transferrin. Similarly, while the lung was heavily populated by GFP-TfR1$^{-/-}$ cells, the tips of the airway had the fewest GFP-TfR1$^{-/-}$ cells compared with stalks or mesenchyme (Supplemental Figure 4). Because the expression of TfR1 has historically been linked to stages of cell proliferation (Kanayasu-Toyoda et al., 1999; Sposi et al., 2000; Wingert et al., 2004), it is tempting to propose that the high proliferative rate of tip cells in kidney and in lung (Michael and Davies, 2004; Nogawa et al 1998; Mollard et al 1998) demands transferrin. While this model is compelling because TfR1 is prominent in branching epithelia, this hypothesis requires testing by measuring the relative proliferative rates of different cell types at different stages in vivo and direct correlation with the level of Tfr1 expression.

In sum, we have utilized a deletion of TfR1 to study iron transport in embryonic kidney. This analysis was possible because the second transferrin receptor (TfR2) had limited or no expression in the kidney as demonstrated by our gene arrays and by in situ hybridization (not shown). The data indicate that Tf-TfR1 targets specific compartments rather than every cell type. Transferrin is captured and required by the ureteric bud tip after E11 but it is not required by metanephric mesenchyme and is poorly internalized and not required by stromal and capsular cells. We identified a novel ferritin receptor and suggest that this pathway may support growth of kidney cells, not only in capsule, but potentially in adjacent mesenchymal cells as well, hence bypassing an overt requirement for TfR1.

Materials and Methods

TfR1 Knockout Embryos

$TfR1^{+/-}$ mice (Levy et al., 1999) were bred with C57BL/6J for five generations and the alleles detected using radio- or 5′ Fam- labelled primers (Invitrogen) as described (Levy et al., 1999).

GFP-$TfR^{-/-}$ ES Cells and Chimeric Embryos

The ROSA26-eGFP knockin construct (Srinivas et al., 2001) was reconstructed with a puromycin selectable marker and introduced into $Tfr1^{-/-}$ ES clones (H5, E12; Ned et al., 2003). 192 puromycin resistant (250 μg/ml) colonies were screened by Southern blot, by anti-CD71 (BD Pharmingen) and by Alexa-568-holo-transferrin (20 μg/ml, 1hr) endocytosis.

Chimeras were generated by introducing 3–5 GFP-$TfR1^{-/-}$ or $Tfr1^{+/+}$ ES cells into wild type C57BL/6 blastocysts. Chimeric tissues were analyzed in permeabilized cryosections (0.1% Triton X-100/0.2%BSA in PBS for 15min at RT) with antibodies to pan Cytokeratin (1:300; Sigma), Pax-2 (1:100; Zymed), Podocalyxin (1:300; R&D System), and Phospho-Histone3 (1:50; Cell Signaling Technology). Alternatively, permeabilized cryosections (0.1% Triton X-100 and 0.5% Saponin in PBS for 1hr with 1% heat inactivated horse serum at RT) were immunoassayed with E-Cadherin (1:400; R&D Systems), Tenascin (1:400; Chemicon), TROMA-1 (1:20; Developmental Studies Hybridoma Bank), active Caspase-3 (1:250; Promega) and ferritin (1:250; Biogenesis) antibodies.

Microarray analysis of GFP-$TfR1^{-/-}$ kidney cells

Chimeric E15 kidneys from two independent litters were digested with collagenase (30 min) and trypsin (5min), quenched with DMEM with 10% FCS, and 10^6 GFP-$TfR1^{-/-}$ or $TfR1^{+/+}$ cells collected by FACS. Total RNA (50ng) was biotin labeled using the Ovation Biotin System (NuGen) and cDNA (2.2 μg) was hybridized in duplicate to Mouse Genome 430 2.0 Genechip arrays (Affymetrix). Image files were analyzed by robust multichip analysis.

Real-Time PCR amplification of Scara5 utilized forward (5′ tggggctgtatcttctggtc3′) and reverse (5′ atcctgaaccttccacacct3′) primers and iQ™ SYBR® Green Super Mix (Biorad), cycled 95° C/2min, and 95°C/30 s and 60°C/30s X 50cycles. Specificity was checked by melting curve analysis and electrophoresis. Scara5 expression was normalized to β-actin expression (forward 5′ ctaaggccaaccgtgaaaag3′ and reverse 5′ tctcagctgtggtggtgaag3′ primers) by ΔC_T method.

Generation of CMV-Scara5-V5 Expressing Cell lines

Full length scara5 cDNA was cloned from mouse E15 Clontech cDNA library by using a forward 5′ caccatggacaacaaagc3′ and reverse 5′ ggggacagtacaagtcac3′ primers and pcDNA3.1 Directional TOPO Expression plasmid. Scara5-V5 was then amplified with primers 5′ gcggatccatggacaacaaagccatgtac-3′ that included a BamH1 site, and 5′

gcgtttaaactcacgtagaatcgagaccgag-3′ that included a PmeI site followed by ligation to pcDNA3.1^{+}.

Trvb cells (a kind gift of McGraw et al., 1987) and MSC-1 cells (a kind gift of McGuinness et al., 1999) were transfected with Scara5, selected with G418 (400 μg/ml) and authenticated by anti-V5 immunoblots (1:5,000 Invitrogen) or immunofluorescence (1:2,000). Ferritin mediated growth in serum free culture media was measured in 2×10^4 cells/well (60hrs) using GAPDH immunoblots (Abcam, 1:5,000).

Imunoprecipitation of Ferritin:Scara5 Complexes

Scara5^{+}-Trvb clones were lysed (in 0.5%NP40, DNase I with protease inhibitors), sonicated (10 sec, 4°C), sheared with an insulin syringe 3X and centrifuged (14,000 rpm; 20 min at 4° C). The supernatant was diluted 2-fold, filtered (0.45 μm) and avidin-ferritin (20 μg; Sigma) or equimolar avidin (2.5 μg; Sigma) added (3hrs). Immunoprecipitates were collected with Protein A and G Agarose Beads (10 μl each; Boehringer-Mannheim) coated with V5 or IgG2a isotype-matched antibodies (10 μg, Jackson Immunoresearch) for 3hrs and washed in PBS with Ca, Mg, 0.5% NP40 (5 times). Avidin-ferritin was detected with biotin-HRP (1 μg/ml in 1% BSA in TBST, Jackson Immunoresearch). The reciprocal immunoprecipitation was performed by coating Biotin-Agarose (10 μl) beads with Avidin or Avidin-ferritin and detecting Scara5 by anti-V5 blots.

Binding and Endocytosis of Ferritin

5,6 carboxytetramethyl-rhodamine, Alexa568, and Alexa488 succinimidyl ester (Molecular Probes) coupled apo-ferritin were authenticated by SDS-PAGE after clean-up on a 100KDa cut-off microcon. Cells were incubated (37°C; 30hrs) with fluorescent ferritin (2 μg/ml) and polynucleotides (50 μg/ml) or untagged ferritin (100 fold excess) and fluorescence quantified by BD LSRII flow cytometer and FloJo7.2.2 software. In some cases, cells were co-labeled with fluorescein-dextran (1mg/ml; 3 hrs) followed by overnight washout. Surface binding utilized apo-ferritin (100 μg/ml; 4°C; 2hrs) followed by immunodetection in unpermeabilized cells with anti-ferritin (Biogenesis, 1:200) and anti-V5. ^{59}Fe-ferritin was prepared by incubating apoferritin at a 1:10 ratio with ^{59}Fe in 10mM HCO_3 at 37°C overnight, followed by clean-up on a 100KDa cut-off microcon. ^{59}Fe-ferritin (3×10^4cpm) was added to 24-well plates containing $2X10^4$ cells.

Iron reporter probes were introduced into MSC1 cells by adenoviral mediated gene transfer. E1/E3 deleted type 5 adenoviral expression constructs contained either a 5′ IRE upstream of destabilized ECFP or a 3′ IRE complex downstream of destabilized EYFP. Virus was produced in 293A cells (ViraPower; Invitrogen) and purified on a CsCl step-gradient, followed by dialysis and infected with MOI=10.

KnockDown of Scara5 in MSC-1 Cells

U6 pEntry Vector (Invitrogen) was used to express hairpin RNAs encoding two shRNA sequences unique to Scara5 (nucleotides 434–452 and 1222–1240; GenBank Accession Number: BC016096) from annealed ssDNAs (1 μg/μl; Invitrogen). MSC-1 were transfected with pU6SR5 or pU6LacZ control plasmid, selected with Blasticidin (2 μg/ml) and three anti-Scara5 siRNA oligos (Ambion) were then transfected to increase the interference. Knockdown was quantified by real time PCR, incubation with FITC-ferritin (20 μg/ml; 2hr at 37°C) and analysis by FACS.

In situ hybridization of Transferrin Receptor1 and Scara5

Digoxigenin-labeled (Roche) antisense riboprobes were generated from plasmids encoding TfR1 (1000nt, exon 1–7) and Scara5 (1476nt, exon 1–8). Sections were stained with anti-digoxigenin (Boehringer-Mannheim; 1:5000 dilution; Schmidt-Ott et al., 2005).

Supplementary Material

Refer to Web version on PubMed Central for supplementary material.

Acknowledgments

We thank F. Costantini, C. Mendelsohn, and Q. Al-Awqati for key reagents and advice. We thank the Reviewers for very insightful comments. This work was supported by grants from the Emerald Foundation, the March of Dimes and the NIDDK (Grants DK-55388 and DK-58872) to J. Barasch and the NIHLB (R01-HL51057) to N.C. Andrews. KMS is an Emmy Noether Fellow of the Deutsche Forshungsgemeinschaft, Germany. There are no conflicts of interest.

References

Aisen P. Transferrin receptor 1. Int J Biochem Cell Biol 2004;36:2137–43. [PubMed: 15313461]

Arosio P, Levi S. Ferritin, iron homeostasis, and oxidative damage. Free Radic Biol Med 2002;33:457–63. [PubMed: 12160928]

Bastin J, Drakesmith H, Rees M, Sargent I, Townsend A. Localisation of proteins of iron metabolism in the human placenta and liver. Br J Haematol 2006;134:532–43. [PubMed: 16856887]

Beaumont C, Leneuve P, Devaux I, Scoazec JY, Berthier M, Loiseau MN, Grandchamp B, Bonneau D. Mutation in the iron responsive element of the L ferritin mRNA in a family with dominant hyperferritinaemia and cataract. Nat Genet 1995;11:444–6. [PubMed: 7493028]

Bratlid D, Moe PJ. Hemoglobin and serum ferritin levels in mothers and infants at birth. Eur J Pediatr 1980;134:125–7. [PubMed: 7439198]

Brekelmans P, van Soest P, Llenen PJ, van Ewijk W. Inhibition of proliferation and differentiation during early T cell development by anti-transferrin receptor antibody. Eur J Immunol 1994;24:2896–902. [PubMed: 7957580]

Bretscher MS, Thomson JN. Distribution of ferritin receptors and coated pits on giant HeLa cells. EMBO J 1983;2:599–603. [PubMed: 6138252]

Camp V, Martin P. The role of macrophages in clearing programmed cell death in the developing kidney. Anat Embryol (Berl) 1996;194:341–8. [PubMed: 8896697]

Chen TT, Li L, Chung DH, Allen CD, Torti SV, Torti FM, Cyster JG, Chen CY, Brodsky FM, Niemi EC, Nakamura MC, Seaman WE, Daws MR. TIM-2 is expressed on B cells and in liver and kidney and is a receptor for H-ferritin endocytosis. J Exp Med 2005;202:955–65. [PubMed: 16203866]

Doi T, Higashino K, Kurihara Y, Wada Y, Miyazaki T, Nakamura H, Uesugi S, Imanishi T, Kawabe Y, Itakura H, et al. Charged collagen structure mediates the recognition of negatively charged macromolecules by macrophage scavenger receptors. J Biol Chem 1993;268:2126–33. [PubMed: 8380589]

Dickinson TK, Connor JR. Cellular distribution of iron, transferrin, and ferritin in the hypotransferrinemic (Hp) mouse brain. J Comp Neurol 1995;355:67–80. [PubMed: 7636015]

Dressler GR. The cellular basis of kidney development. Annu Rev Cell Dev Biol 2006;22:509–29. [PubMed: 16822174]

Ekblom P, Thesleff I, Saxen L, Miettinen A, Timpl R. Transferrin as a fetal growth factor: acquisition of responsiveness related to embryonic induction. Proc Natl Acad Sci U S A 1983;80:2651–5. [PubMed: 6405384]

Ferreira C, Santambrogio P, Martin ME, Andrieu V, Feldmann G, Henin D, Beaumont C. H ferritin knockout mice: a model of hyperferritinemia in the absence of iron overload. Blood 2001;98:525–32. [PubMed: 11468145]

Fisher J, Devraj K, Ingram J, Slagle-Webb B, Madhankumar AB, Liu X, Klinger M, Simpson IA, Connor JR. Ferritin: a novel mechanism for delivery of iron to the brain and other organs. Am J Physiol Cell Physiol 2007;293:C641–9. [PubMed: 17459943]

Flo TH, Smith KD, Sato S, Rodriguez DJ, Holmes MA, Strong RK, Akira S, Aderem A. Lipocalin 2 mediates an innate immune response to bacterial infection by sequestrating iron. Nature 2004;432 (7019):917–21. [PubMed: 15531878]

Gelvan D, Fibach E, Meyron-Holtz EG, Konijn AM. Ferritin uptake by human erythroid precursors is a regulated iron uptake pathway. Blood 1996;88:3200–7. [PubMed: 8874221]

Gentili C, Doliana R, Bet P, Campanile G, Colombatti A, Cancedda FD, Cancedda R. Ovotransferrin and ovotransferrin receptor expression during chondrogenesis an endochondral bone formation in developing chick embryo. J Cell Biol 1994;124:579–88. [PubMed: 8106555]

Ghosh S, Hevi S, Chuck SL. Regulated secretion of glycosylated human ferritin from hepatocytes. Blood 2004;103:2369–76. [PubMed: 14615366]

Gunshin H, Fujiwara Y, Custodio AO, Direnzo C, Robine S, Andrews NC. Slc11a2 is required for intestinal iron absorption and erythropoiesis but dispensable in placenta and liver. J Clin Invest 2005;115:1258–66. [PubMed: 15849611]

Gustine D, Zimmerman E. Developmental changes in microheterogeneity of foetal plasma glycoproteins of mice. Biochem J 1973;132:541–551. [PubMed: 4353382]

Hamill RL, Woods JC, Cook BA. Congenital atransferrinemia. A case report and review of the literature. Am J Clin Pathol 1991;96:215–8. [PubMed: 1862777]

Han HJ, Tokino T, Nakamura Y. CSR, a scavenger receptor-like protein with a protective role against cellular damage caused by UV irradiation and oxidative stress. Hum Mol Genet 1998;7:1039–46. [PubMed: 9580669]

Hatini V, Huh SO, Herzlinger D, Soares VC, Lai E. Essential role of stromal mesenchyme in kidney morphogenesis revealed by targeted disruption of Winged Helix transcription factor BF-2. Genes and Dev 1996;10:1467–78. [PubMed: 8666231]

Hayashi A, Wada Y, Suzuki T, Shimizu A. Studies on familial hypotransferrinemia: unique clinical course and molecular pathology. Am J Hum Genet 1993;53:201–13. [PubMed: 8317485]

Huggenvik JI, Craven CM, Idzerda RL, Bernstein S, Kaplan J, McKnight GS. A splicing defect in the mouse transferrin gene leads to congenital atransferrinemia. Blood 1989;74:482–6. [PubMed: 2752125]

Hulet SW, Hess EJ, Debinski W, Arosio P, Bruce K, Powers S, Connor J. Characterization and distribution of ferritin binding sites in the adult mouse brain. J Neurochem 1999;72:868–74. [PubMed: 9930764]

Hulet SW, Heyliger SO, Powers S, Connor JR. Oligodendrocyte progenitor cells internalize ferritin via clathrin-dependent receptor mediated endocytosis. J Neurosci Res 2000;61:52–60. [PubMed: 10861799]

Hussain MA, Gaafar TH, Laulicht M, Hoffebrand AV. Relation of maternal and cord blood serum ferritin. Arch Dis Child 1977;52:782–4. [PubMed: 931424]

Jiang Y, Oliver P, Davies KE, Platt N. Identification and characterization of murine SCARA5, a novel class A scavenger receptor that is expressed by populations of epithelial cells. J Biol Chem 2006;281:11834–45. [PubMed: 16407294]

Kanayasu-Toyoda T, Yamaguchi T, Uchida E, Hayakawa T. Commitment of neutrophilic differentiation and proliferation of HL-60 cells coincides with expression of transferrin receptor. J Biol Chem 1999;274:25471–80. [PubMed: 10464278]

Kanwar YS, Liu ZZ, Kumar A, Wada J, Carone FA. Cloning of mouse c-ros renal cDNA, its role in development and relationship to extracellular matrix glycoproteins. Kidney Int 1995;48:1646–59. [PubMed: 8544427]

Kispert A, Vainio S, Shen L, Rowitch DH, McMahon AP. Proteoglycans are required for maintenance of Wnt-11 expression in the ureter tips. Development 1996;122:3627–37. [PubMed: 8951078]

Kobayashi K. Fine structure of the mammalian renal capsule: the atypical smooth muscle cell and its functional meaning. Cell Tissue Res 1978;195:381–94. [PubMed: 728976]

Koseki C, Herzlinger D, al-Awqati Q. Apoptosis in metanephric development. J Cell Biol 1992;119:1327–33. [PubMed: 1447305]

Lamparelli RD, Friedman BM, MacPhail AP, Bothwell TH, Phillips JI, Baynes RD. The fate of intravenously injected tissue ferritin in pregnant guinea-pigs. Br J Haematol 1989;72:100–5. [PubMed: 2736234]

Leimberg MJ, Prus E, Konijn AM, Fibach E. Macrophages function as a ferritin iron source for cultured human erythroid precursors. J Cell Biochem 2008;103:1211–8. [PubMed: 17902167]

Levinson R, Mendelsohn C. Stromal progenitors are important for patterning epithelial and mesenchymal cell types in the embryonic kidney. Semin Cell Dev Biol 2003;14:225–31. [PubMed: 14627121]

Levy JE, Jin O, Fujiwara Y, Kuo F, Andrews NC. Transferrin receptor is necessary for development of erythrocytes and the nervous system. Nat Genet 1999;21:396–9. [PubMed: 10192390]

Levi S, Luzzago A, Cesareni G, Cozzi A, Franceschinelli F, Albertini A, Arosio P. Mechanism of ferritin iron uptake: activity of the H-chain and deletion mapping of the ferro-oxidase site. J Biol Chem 1988;263:18086–92. [PubMed: 3192527]

Levi S, Salfeld J, Franceschinelli F, Cozzi A, Dorner MH, Arosio P. Expression and structural and functional properties of human ferritin L-chain from Escherichia coli. Biochemistry 1989;28:5179–84. [PubMed: 2669970]

Levi S, Yewdall SJ, Harrison PM, Santambrogio P, Cozzi A, Rovida E, Albertini A, Arosio P. Evidence of H- and L-chains have co-operative roles in the iron-uptake mechanism of human ferritin. Biochem J 1992;288:591–6. [PubMed: 1463463]

Levi S, Santambrogio P, Cozzi A, Rovida E, Corsi B, Tamborini E, Spada S, Albertini A, Arosio P. The role of the L-chain in ferritin iron incorporation. Studies of homo and heteropolymers. J Mol Biol 1994;238:649–54. [PubMed: 8182740]

Li JY, Ram G, Gast K, Chen X, Barasch K, Mori K, Schmidt-Ott K, Wang J, Kuo HC, Savage-Dunn C, Garrick MD, Barasch J. Detection of intracellular iron by its regulatory effect. Am J Physiol Cell Physiol 2004;287:C1547–59. [PubMed: 15282194]

Linder MC, Schaffer KJ, Hazegh-Azam M, Zhou CY, Tran TN, Nagel GM. Serum ferritin: does it differ from tissue ferritin? J Gastroenterol Hepatol 1996;11:1033–6. [PubMed: 8985824]

Macedo MF, de Sousa M, Ned RM, Mascarenhas C, Andrews NC, Correia-Neves M. Transferrin is required for early T-cell differentiation. Immunology 2004;112:543–9. [PubMed: 15270724]

Mack U, Powell LW, Halliday JW. Detection and isolation of a hepatic membrane receptor for ferritin. J Biol Chem 1983;258:4672–5. [PubMed: 6300097]

MacPhail AP, Charlton RW, Bothwell TH, Torrance JD. The relationship between maternal and infant iron status. Scand J Haematol 1980;25:141–50. [PubMed: 7466303]

Marose TD, Merkel CE, McMahon AP, Carroll TJ. Beta-catenin is necessary to keep cells of ureteric bud/Wolffian duct epithelium in a precursor state. Dev Biol 2008;314:112–26. [PubMed: 18177851]

McGraw TE, Greenfield L, Maxfield FR. Functional expression of the human transferrin receptor cDNA in Chinese hamster ovary cells deficient in endogenous transferrin receptor. J Cell Biol 1987;105:207–14. [PubMed: 3611186]

McGuinness MP, Linder CC, Morales CR, Heckert LL, Pikus J, Griswold MD. Relationship of a mouse Sertoli cell line (MSC-1) to normal Sertoli cells. Biol Reprod 1994;51:116–24. [PubMed: 7918865]

Michael L, Davies JA. Pattern and regulation of cell proliferation during murine ureteric bud development. J Anat 2004;204:241–55. [PubMed: 15061751]

Mollard R, Dziadek M. A correlation between epithelial proliferation rates, basement membrane component localization patterns, and morphogenetic potential in the embryonic mouse lung. Am J Respir Cell Mol Biol 1998;19(1):71–82. [PubMed: 9651182]

Moss D, Powell LW, Arosio P, Halliday JW. Characterization of the ferritin receptors of human T lymphoid (MOLT-4) cells. J Lab Clin Med 1992;119:273–9. [PubMed: 1311740]

Meyron-Holtz EG, Vaisman B, Cabantchik ZI, Fibach E, Rouault TA, Hershko C, Konijn AM. Regulation of intracellular iron metabolism in human erythroid precursors by internalized extracellular ferritin. Blood 1999;94:3205–11. [PubMed: 10556209]

Ned RM, Swat W, Andrews NC. Transferrin receptor 1 is differentially required in lymphocyte development. Blood 2003;102:3711–8. [PubMed: 12881306]

Nogawa H, Morita K, Cardoso WV. Bud formation precedes the appearance of differential cell proliferation during branching morphogenesis of mouse lung epithelium in vitro. Dev Dyn 1998;213 (2):228–35. [PubMed: 9786423]

Ohgami RS, Campagna DR, Greer EL, Antiochos B, McDonald A, Chen J, Sharp JJ, Fujiwara Y, Barker JE, Fleming MD. Identification of a ferrireductase required for efficient transferrin-dependent iron uptake in erythroid cells. Nat Genet 2005;37:1264–9. [PubMed: 16227996]

Ojala JR, Pikkarainen T, Tuuttila A, Sandalova T, Tryggvason K. Crystal structure of the cysteine-rich domain of scavenger receptor MARCO reveals the presence of a basic and an acidic cluster that both contribute to ligand recognition. J Biol Chem 2007;282:16654–66. [PubMed: 17405873]

Orlic D, Lev R, Rosenthal WS. Fetal rat utilization of 55Fe absorbed by fetal intestine from swallowed amniotic fluid. Blood 1974;43:429–36. [PubMed: 4811825]

Ponka P, Beaumont C, Richardson DR. Function and regulation of transferrin and ferritin. Semin Hematol 1998;35:35–54. [PubMed: 9460808]

Puolakka J, Janne O, Pakarinen A, Vihko R. Serum ferritin in the diagnosis of anemia during pregnancy. Acta Obstet Gynecol Scand Suppl 1980;95:57–63. [PubMed: 6935913]

Qiu A, Jansen M, Sakaris A, Min SH, Chattopadhyay S, Tsai E, Sandoval C, Zhao R, Akabas MH, Goldman ID. Identification of an intestinal folate transporter and the molecular basis for hereditary folate malabsorption. Cell 2006;127:917–28. [PubMed: 17129779]

Rae F, Woods K, Sasmono T, Campanale N, Taylor D, Ovchinnikov DA, Grimmond SM, Hume DA, Ricardo SD, Little MH. Characterisation and trophic functions of murine embryonic macrophages based upon the use of a Csf1r-EGFP transgene reporter. Dev Biol 2007;308:232–46. [PubMed: 17597598]

Radisky DC, Kaplan J. Iron in cytosolic ferritin can be recycled through lysosomal degradation in human fibroblasts. Biochem J 1998;336:201–5. [PubMed: 9806901]

Recalcati S, Invernizzi P, Arosio P, Cairo G. New functions for an iron storage protein: the role of ferritin in immunity and autoimmunity. J Autoimmun 2008;30:84–9. [PubMed: 18191543]

San Martin CD, Garri C, Pizarro F, Walter T, Theil EC, Núñez MT. Caco-2 intestinal epithelial cells absorb soybean ferritin by mu2 (AP2)-dependent endocytosis. J Nutr 2008;138:659–66. [PubMed: 18356317]

Schmidt-Ott KM, Yang J, Chen X, Wang H, Paragas N, Mori K, Li JY, Lu B, Costantini F, Schiffer M, Bottinger E, Barasch J. Novel regulators of kidney development from the tips of the ureteric bud. J Am Soc Nephrol 2005;16:1993–2002. [PubMed: 15917337]

Schmidt-Ott KM, Chen X, Paragas N, Levinson RS, Mendelsohn CL, Barasch J. c-kit delineates a distinct domain of progenitors in the developing kidney. Dev Biol 2006;299:238–49. [PubMed: 16942767]

Sibille JC, Ciriolo M, Kondo H, Crichton RR, Aisen P. Subcellular localization of ferritin and iron taken up by rat hepatocytes. Biochem J 1989;262:685–8. [PubMed: 2803277]

Siddappa AJ, Rao RB, Wobken JD, Leibold EA, Connor JR, Georgieff MK. Developmental changes in the expression of iron regulatory proteins and iron transport proteins in the perinatal rat brain. J Neurosci Res 2002;68:761–75. [PubMed: 12111837]

Siddappa AM, Rao R, Long JD, Widness JA, Georgieff MK. The assessment of newborn iron stores at birth: a review of the literature and standards for ferritin concentrations. Neonatology 2007;92:73–82. [PubMed: 17361090]

Simpson RJ, Raja KB, Halliwell B, Evans PJ, Aruoma OI, Konijn AM, Peters TJ. Iron speciation in hypotransferrinaemic mouse serum. Biochem Soc Trans 1991;19:317S. [PubMed: 1783153]

Sposi N, Cianetti L, Tritarelli E, Pelosi E, Militi S, Barberi T, Gabbianelli M, Saulle E, Kuhn L, Peschle C, Testa U. Mechanisms of differential transferrin receptor expression in normal hematopoiesis. Eur J Biochem 2000;267:6762–74. [PubMed: 11082186]

Srinivas S, Goldberg MR, Watanabe T, D'Agati V, al-Awqati Q, Costantini F. Expression of green fluorescent protein in the ureteric bud of transgenic mice: a new tool for the analysis of ureteric bud morphogenesis. Dev Genet 1999;24:241–51. [PubMed: 10322632]

Srinivas S, Watanabe T, Lin CS, William CM, Tanabe Y, Jessell TM, Costantini F. Cre reporter strains produced by targeted insertion of EYFP and ECFP into the ROSA26 locus. BMC Dev Biol 2001;1:4. [PubMed: 11299042]

Thorstensen K, Trinder D, Zak O, Aisen P. Uptake of iron from N-terminal half-transferrin by isolated rat hepatocytes. Evidence of transferrin-receptor-independent iron uptake. Eur J Biochem 1995;232:129–33. [PubMed: 7556141]

Tran TN, Eubanks SK, Schaffer KJ, Zhou CY, Linder MC. Secretion of ferritin by rat hepatoma cells and its regulation by inflammatory cytokines and iron. Blood 1997;90:4979–86. [PubMed: 9389717]

Trenor CC 3rd, Campagna DR, Sellers VM, Andrews NC, Fleming MD. The molecular defect in hypotransferrinemic mice. Blood 2000;96:1113–8. [PubMed: 10910930]

Watanabe K, Yamashita Y, Ohgawara H, Sekiguchi M, Satake N, Orino K, Yamamoto S. Iron content of rat serum ferritin. J Vet Med Sci 2001;63:587–9. [PubMed: 11411511]

Wingert RA, Brownlie A, Galloway JL, Dooley K, Fraenkel P, Axe JL, Davidson AJ, Barut B, Noriega L, Sheng X, Zhou Y, Zon LI. The chianti zebrafish mutant provides a model for erythroid-specific disruption of transferrin receptor1. Development 2004;131:6225–35. [PubMed: 15563524]

Xu J, Ling EA. Studies of the ultrastructure and permeability of the blood-brain barrier in the developing corpus callosum in postnatal rat brain using electron dense tracers. J Anat 1994;184:227–37. [PubMed: 8014116]

Yuan XM, Li W, Baird SK, Carlsson M, Melefors O. Secretion of ferritin by iron-laden macrophages and influence of lipoproteins. Free Radic Res 2004;38:1133–42. [PubMed: 15512802]

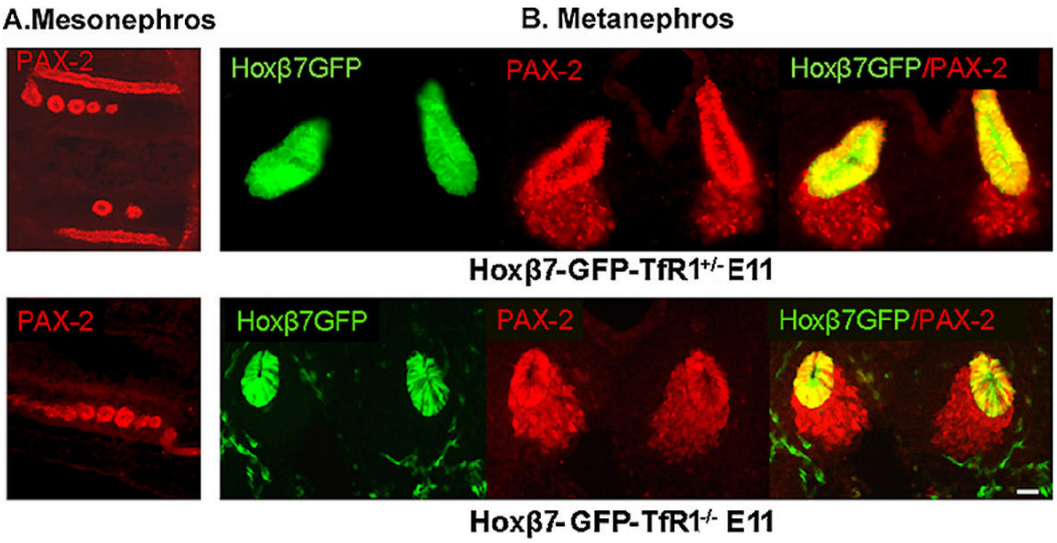

Figure 1.

Initial stages of renal development were preserved in TfR1$^{-/-}$ mice. (A) Pax2^{+} Wolffian ducts and mesonephros and (B) Pax2^{+} ureteric buds surrounded by mesenchymal cells were detected in TfR1$^{-/-}$ E11 embryos. Crosses with Hoxβ7-GFP mice distinguished the ureteric bud (GFP^{+}Pax-2^{+}) from mesenchyme (GFP^{-}Pax-2^{+}). Bar=10 μm.

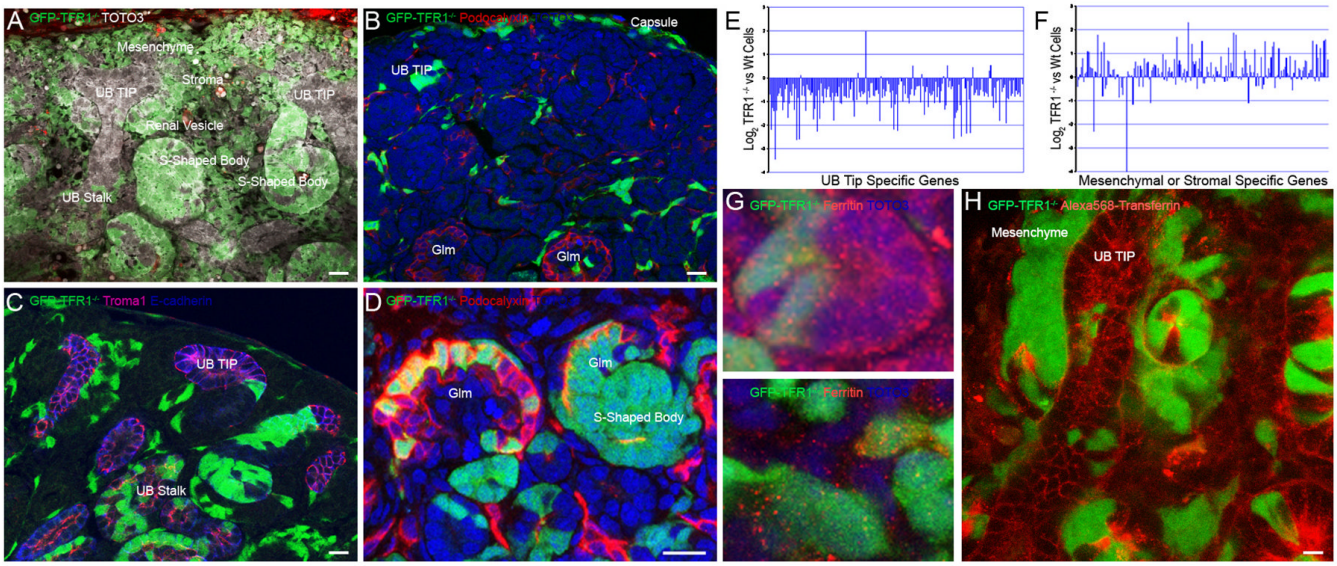

Figure 2.

Development of GFP-TfR1$^{-/-}$ cells in E15 kidney. (A) GFP-TfR1$^{-/-}$ cells were readily detected in capsule and stroma, mesenchyme, renal vesicles, and S-shaped bodies, but detected with limited frequency in UB tips (bar=10 μm). (B) GFP-TfR1$^{-/-}$ cells (42%) reside in the capsule, interstitium, and podocalyxin^{+} vascular progenitors (confocal section; bar=10 μm). (C, D) GFP-TfR1$^{-/-}$ cells (58%) also resided in proximal and distal nephrons (Ecadherin^{+}; dark blue), in podocytes (podocalyxin^{+}; red, Glm=glomerulus) and in the UB stalk (Ecadherin^{+}, dark blue; Troma^{+}, pink). In some cases, entire segments of the S-shaped body were composed of GFP-TfR1$^{-/-}$ cells (confocal section; bar=10 μm). (E, F) Genes specific for UB tip or mesenchymal-stromal compartments were assayed in GFP-TfR1$^{-/-}$ and wild type cells and presented as the $\log_2$ ratio of microarray values. UB tip specific genes were under represented in GFP-TfR1$^{-/-}$ cells, whereas mesenchymal-stromal genes were expressed. (G) Both GFP-TfR1$^{-/-}$ and wild type cells (two sections are shown) contained cytoplasmic ferritin. (H) Wild type cells captured Alexa568-transferrin, but neighboring GFP-TfR1$^{-/-}$ were unlabeled. Bar=10 μm.

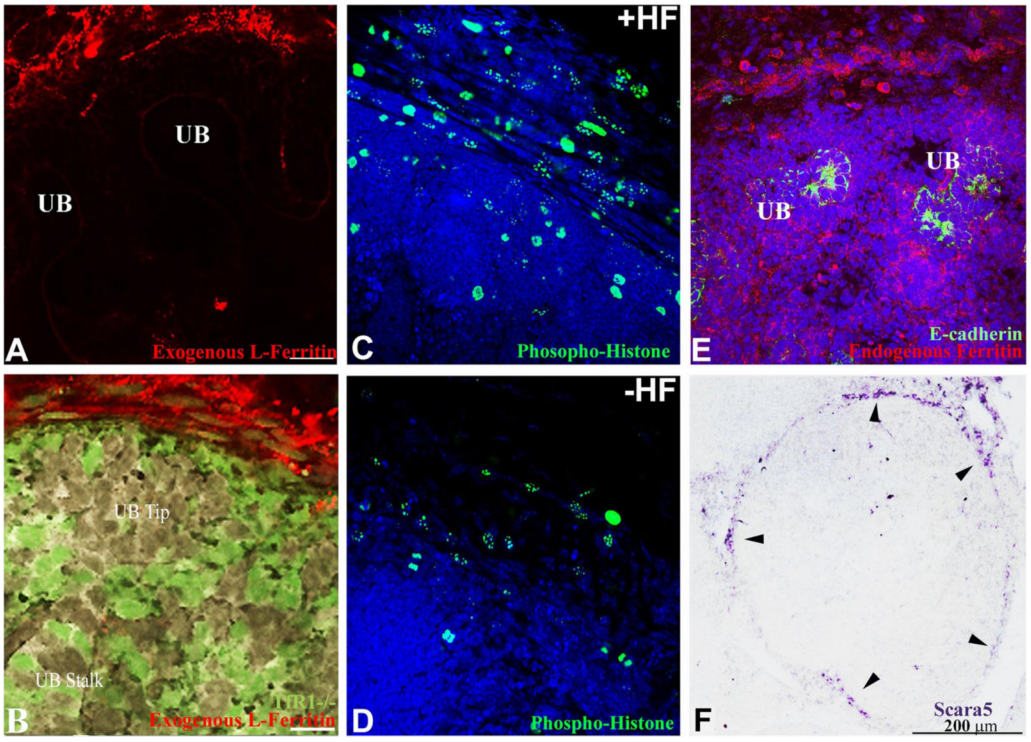

Figure 3.

Ferritin capture, cell proliferation and Scara5 expression in the capsule of the E15 kidney. (A, B) Both wild type and GFP-TfR1$^{-/-}$ capsular cells captured rhodamine coupled “Exogenous L-Ferritin”. Bars=20 μm. (C) Holoferritin (+HF; 1.25 μg/ml) induced phosphohistone^{+} nuclei and expanded layers of capsular cells, (D) whereas culture with apoferritin (−HF; 1.25 μg/ml) failed to preserve the capsule. (E) “Endogenous Ferritin” was present throughout the kidney, particularly in the capsule. E-cadherin marked the UB. (F) Scara5 RNA was expressed by spindle-shaped cells encapsulating the kidney (arrowheads) and more faintly by cortical stroma.

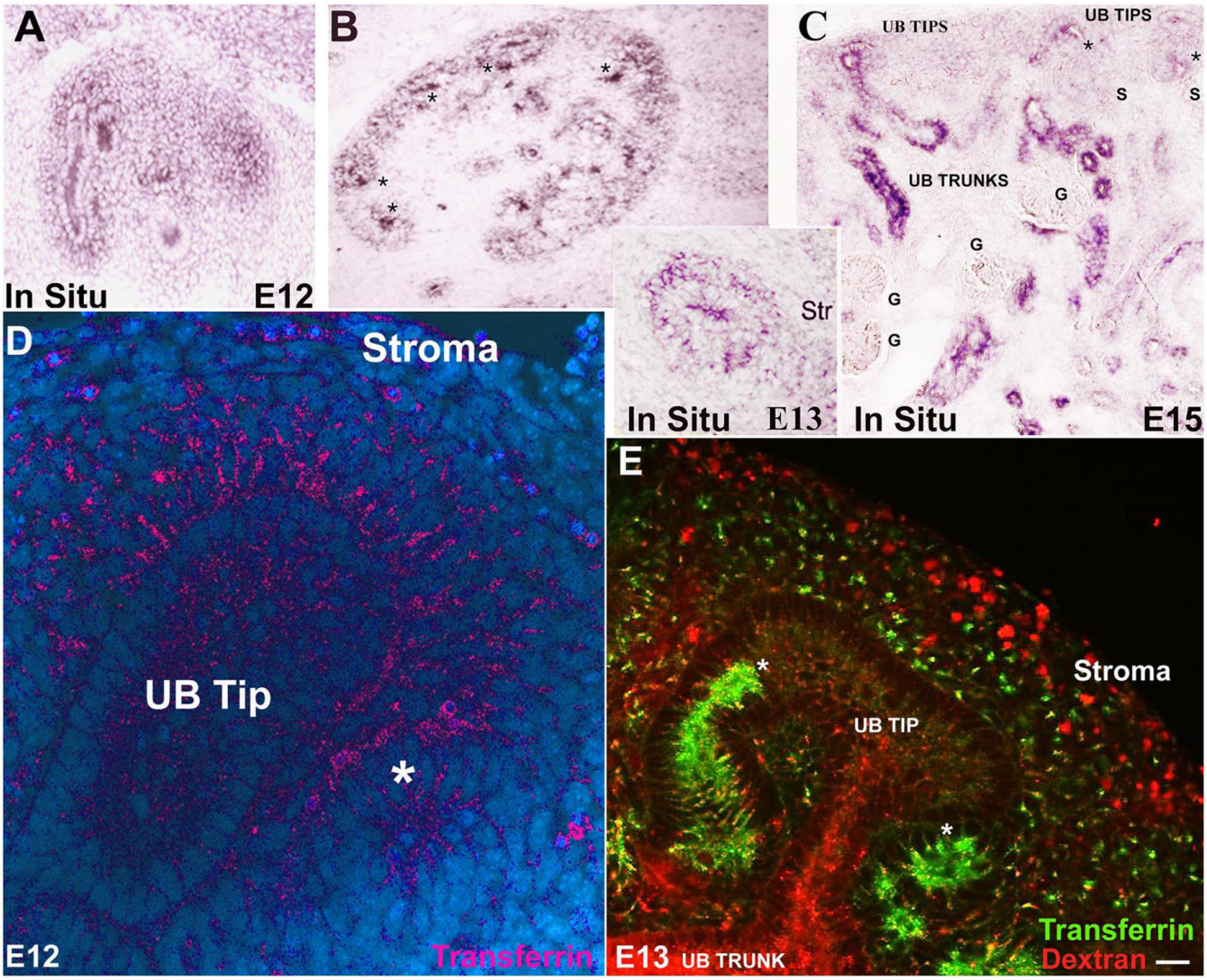

Figure 4.

Localization of the transferrin pathway. (A, B, C) TfR1 was initially localized to UB tips and cap mesenchyme. By E13, renal vesicles also expressed TfR1 (*B, C). TfR1 expression was reduced or absent in glomeruli ("G"), stroma and capsule. (D) Rhodamine- and (E) fluorescein-transferrin endocytosis paralleled TfR1 expression. Stroma and capsule were weakly labeled despite active fluid-phase endocytosis (rhodamine-dextran; E). (*Presumptive distal nephron; Bar= 10 μm).

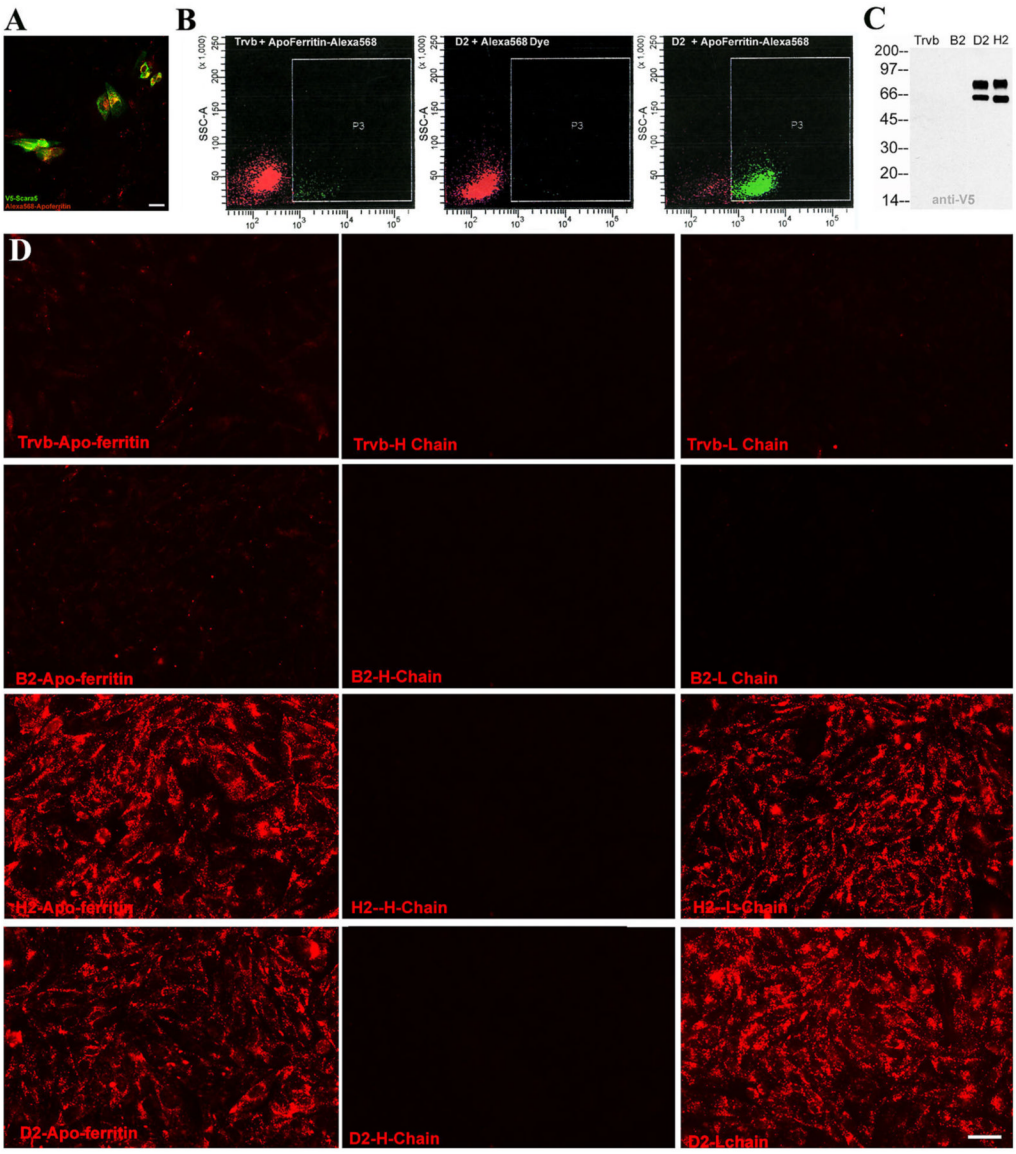

Figure 5.

Interaction between Scara5 and L-ferritin. (A) Transient transfection of Scara5-V5 (anti-V5, green) and (B) stable expression of Scara5-V5 resulted in the capture of Alexa568-ferritin (A, B right panel) whereas parental Trvb, which are Scara5^{-}TfR1^{-} cells, transfected with an empty vector were negative (B left panel). Tris-quenched Alexa568 dye (no ferritin) was an additional control (middle panel). (C) Expression of Scara5-V5 (59KDa, 70KDa) was detected by V5 monoclonal antibody. (D) Endocytosis of Alexa568-ferritin was analyzed in Scara5^{-} (Trvb, B2 clones) and Scara5^{+} (D2 and H2) stable clones. Nearly all D2 and H2 cells captured apo- and L-ferritins, but not H-ferritin. Bar=10 μm.

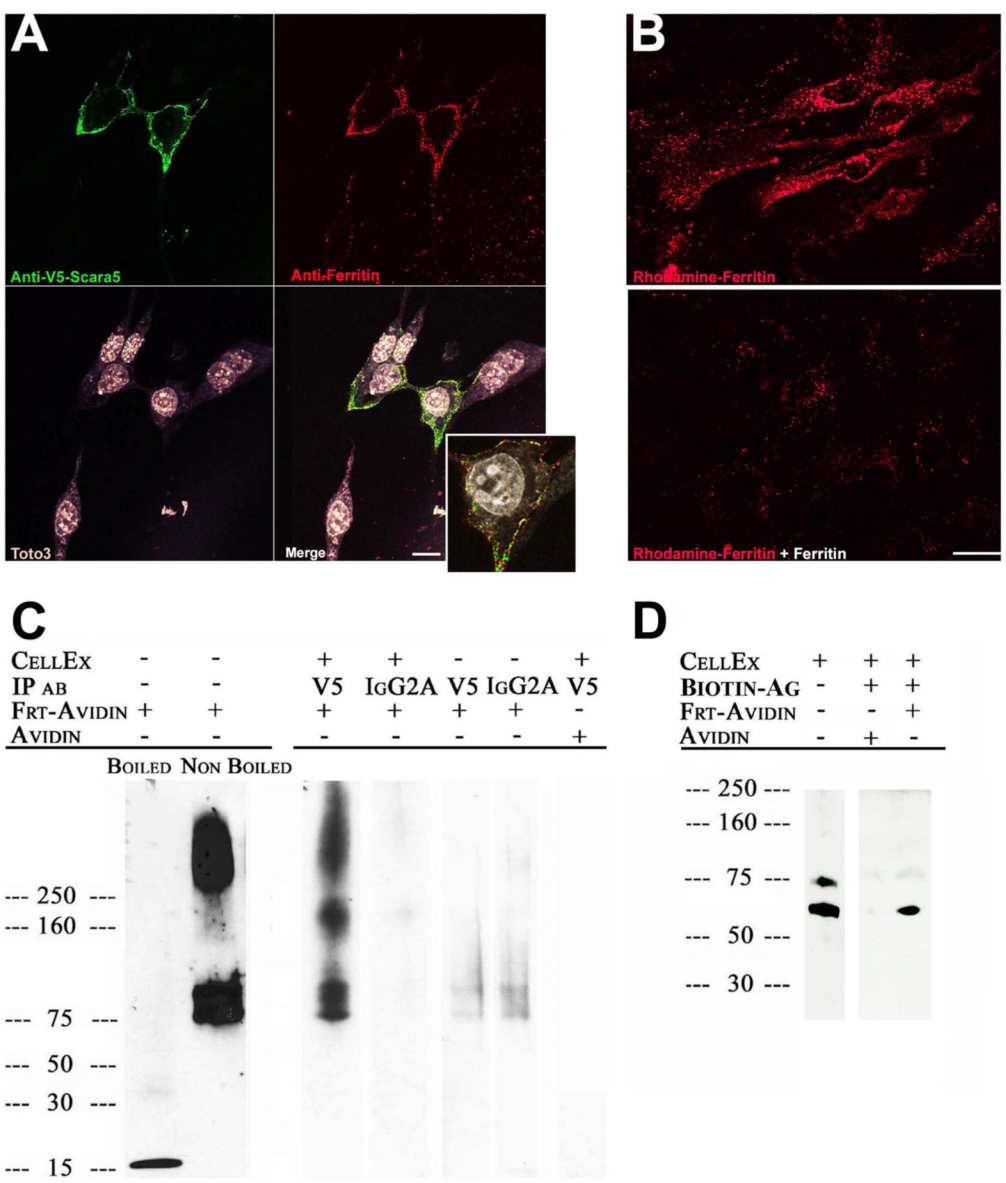

Figure 6.

Interaction between Scara5 and ferritin at the cell surface. (A) Scara5-V5 (anti-V5; Cy2; green) and ferritin (anti-ferritin; Cy3; red) co-localized at the surface (Z-stack; inset: single confocal section) of Scara5-V5 transfected MSC-1 cells incubated with untagged ferritin (2hrs; 4°C). Toto3 marked nuclei. Bar=10 μm. (B) Endocytosis of rhodamine-ferritin (30hrs; 37°C; top panel) was blocked by a 100 fold excess untagged ferritin (bottom panel), Bar=20 μm. (C) V5 antibodies precipitated Scara5-V5 with avidin tetramer-ferritin monomer (85KDa) or multimers (200KDa, >250KDa), but not with unconjugated avidin. Irrelevant isotype matched antibodies did not immunoprecipitate ferritin-avidin nor were ferritin-avidin complexes recovered without cell extracts. (D) Scara5-V5 was detected in cell extracts (clone D2) and in pull-downs with ferritin-avidin-biotin-agarose beads but not with avidin-biotin-agarose-beads.

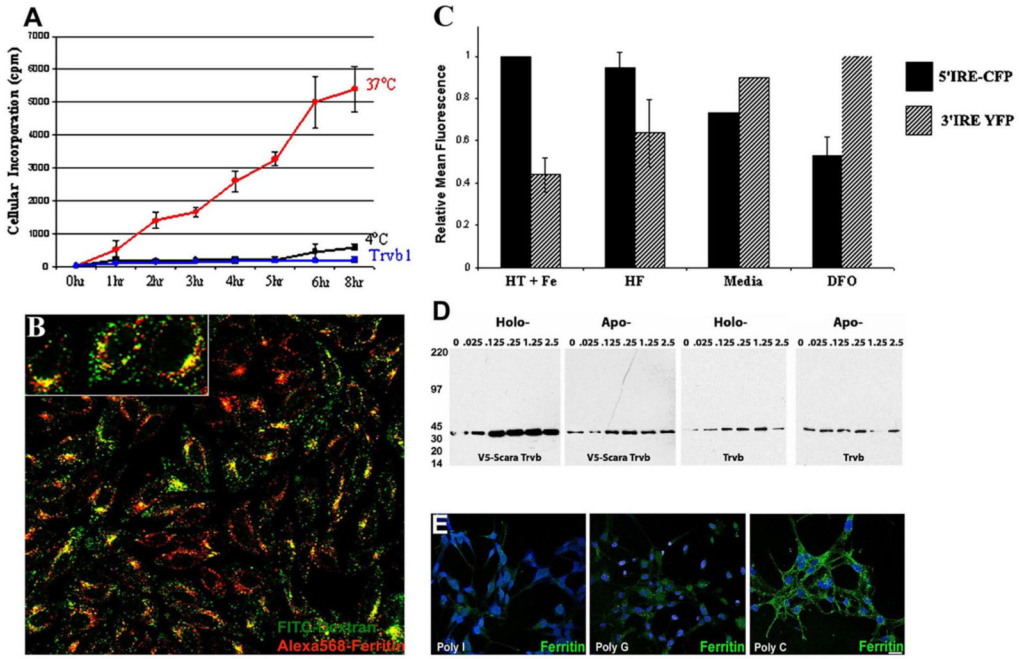

Figure 7.

Scara5 mediates cellular uptake of ferritin-bound iron and represents an endogenous pathway in MSC-1 cells. (A) Capture of ^{59}Fe-ferritin by Scara5^{+} at 37°C (red line) but not at 4°C (black line) nor by parental Trvb cells (blue line). (B) Lysosomes of Scara5^{+} Trvb cells were marked with fluorescein-dextran (green). They contained endocytosed Alexa568-ferritin (red). Original magnification 40X. (C) Transfer of iron to the cytoplasm was detected using two IRE-based iron reporters and FACS analysis in MSC-1 cells. The maximal 5′ IRE-CFP signal (designated 100%-black bars) was generated by iron loading with holotransferrin (20 μg/ml) and ferric ammonium citrate (20 μM) (HT+Fe) and the maximal 3′ IRE-YFP signal (designated 100%-stippled bars) was generated by DFO (20 μM). These treatments produced a ~7-fold range in the ratio of 5′/3′ IRE signals. Treatment with holoferritin (HF) increased 5′ IRE-CFP but decreased the 3′ IRE-YFP signal. (D) Holoferritin induces cell growth. Scara5^{+} clone H responded to holo- but not to apo-ferritin, whereas Trvb cells failed to respond. Cell protein was detected by GAPDH immunoblots. (E) Alexa488-ferritin endocytosis was blocked by Poly I >Poly G >Poly C (50 μM). Similar data were obtained in Scara5^{+} Trvb and MSC1 cells. Bar=20 μM.